

Higher Order Composite DG approximations of Gross–Pitaevskii ground state: benchmark results and experiments

C. Engström¹, S. Giani², L. Grubišić^{3,*}

Abstract

Discontinuous Galerkin composite finite element methods (DGCFEM) are designed to tackle approximation problems on complicated domains. Partial differential equations posed on complicated domain are common when there are mesoscopic or local phenomena which need to be modeled at the same time as macroscopic phenomena. In this paper, an optical lattice will be used to illustrate the performance of the approximation algorithm for the ground state computation of a Gross-Pitaevskii equation, which is an eigenvalue problem with eigenvector nonlinearity. We will adapt the convergence results of Marcati and Maday 2018 to this particular class of discontinuous approximation spaces and benchmark the performance of the classic symmetric interior penalty hp-adaptive algorithm against the performance of the hp-DGCFEM.

Keywords: Gross – Pitaevskii eigenvalue problem, discontinuous Galerkin finite element approximations, composite finite elements

2020 MSC: 65N35, 65M60, 78M10

1. Introduction

This paper presents a higher order discretization method for finding the ground state of nonlinear eigenvalue problems of Gross-Pitaevskii type. Our prototype model problem is to find the smallest positive scalar λ and a function u such that

$$\begin{cases} -\Delta u + bu + F(|u|^2)u = \lambda u, & \text{in } \Omega \\ \|u\|_2 = 1, \\ u = 0, & \text{on } \partial\Omega. \end{cases} \quad (1)$$

The real function F is assumed to be convex, and smooth with further restrictions posed on its growth to ensure the compactness of a certain operator resolvent, see [14]. The

*Corresponding author

Email addresses: christian.engstrom@lnu.se (C. Engström), stefano.giani@durham.ac.uk (S. Giani), luka.grubisic@math.hr (L. Grubišić)

¹Department of Mathematics, Faculty of Technology, Linnaeus University, Sweden

²Durham University, Department of Engineering, South Rd, Durham, DH13LE, United Kingdom

³Department of Mathematics, Faculty of Science, University of Zagreb, Bijenička 30, 10000 Zagreb, Croatia

domain Ω will be a Lipschitz domain in \mathbb{R}^2 and we will assume that either the domain Ω or the function b exhibit features which need to be modeled by a hierarchy of adaptively refined meshes. We are interested in composite finite element approximation methods, which recursively combine information from all of the resolution (refinement) levels, much like a multigrid method would, to compute approximations which describe both macroscopic and microscopic/mesososcopic parts of the solution. As a terminological convention we call the operator defined by the formal expression $H = -\Delta + b$ the Schrödinger Hamiltonian and the scalar function b is called the potential.

Models from the family (1) are used to analyze Bose-Einstein condensates, [13, 36, 37]. A Bose-Einstein condensate is a state of the matter created when the de Broglie wavelength of a gas of bosons is larger than the average inter-particle spacing, leading to a macroscopic occupation of a single quantum state. This is a low temperature phase transition that is only accessible to bosons. The mean-field theory describing Bose-Einstein Condensates (BECs) at zero temperature is given by the Gross Pitaevskii (GP) equation, which is an equation of the type (1).

The potential b describes the outer influence which confines the system (gas of bosons). The nonlinear part of the equation describes the two-body interactions between the particles. Our primary motivation is to study effective potentials from the class of optical lattices. These are artificial crystals of light created by interfering optical laser beams. When atoms are illuminated with laser beams, the electric field of the laser induces a dipole moment in the atoms which in turn interacts with the electric field. This interaction modifies the energy of the internal states of the atoms in a way that depends both on the light intensity and on the laser frequency. A spatially dependent intensity induces a spatially dependent potential energy which can be used to trap the atoms. An optical lattice is the periodic potential energy landscape that the atoms experience as a result of the standing wave pattern generated by the interference of laser beams.

A typical approach to dealing with Gross-Pitaevskii type eigenvalue problems is either through the use of Fourier approximation methods such as in [5] or through the use of spectral discretization [12, 34]. Recently, non-local effects in the model are studied through the use of equations based on fractional derivatives [33]. It is known that a Fourier or spectral discretization approach might face convergence slowdowns when encountering the effects of a local, difficult to resolve, structure. Our approach is to achieve the spectral accuracy by using high order composite finite element methods which are specifically tailored to account for the effects of a finer local structure while retaining high performance. Our experiments will show a numerical method with the observed exponential convergence.

The particular challenge for this study will be modeling such potentials b using a hierarchy of meshes such that the computational complexity scale with the macroscopic resolution step size rather than with the microscopic scale resolution step-size. We base our approach on the composite finite element discretizations of [16] and use the recent results of [29] to justify the convergence of our method. We note that the idea of using composite finite elements is quite old. In this work, we were particularly influenced by the work of Hackbusch and Sauter [22, 23, 21], where further references can be found.

This paper is organized as follows. In Section 2 we present the mathematical analysis of the problem and emphasize the role played by the convexity and the smoothness properties of the energy functional. Moreover, we review basic convergence results from [29]. In Sections 3 and 4 we review basic conventions of high order discontinuous Galerkin finite element approximation methods and present results on the convergence of the proposed method. Also we outline the implementation details. Finally in Section 5 we present extensive numerical experiments and provide benchmark results for certain types of confining potentials.

2. Analysis of the model problem

Pioneering work on the numerical analysis of the eigenvalue problem (1) was done by Zhou [11]. Here, we base our analysis on the approach of Maday and coworkers from [11]. The ground state of the eigenvalue problem

$$\begin{cases} -\Delta u + bu + \beta|u|^2u = \lambda u, & \text{in } \Omega \\ u = 0, & \text{on } \partial\Omega \\ \|u\|_2 = 1. \end{cases} \quad (2)$$

can be computed as the positive solution of the following convex constrained optimization problem

$$u_* = \arg\text{-min}\{E(v) : v \in X, \|u\|_{L^2} = 1\}. \quad (3)$$

Here the space $X \subset L^2(\Omega)$ is the form domain – in the sense of Kato [27]– of the Schrödinger Hamiltonian $H = -\Delta + b$ and the functional $E : X \rightarrow \mathbb{R}$ is defined by the formula

$$E(\psi) = \frac{1}{2} \int_{\Omega} \nabla\psi \cdot \nabla\psi \, dV + \frac{1}{2} \int_{\Omega} b \psi^2 \, dV + \frac{\beta}{4} \int_{\Omega} \psi^4 \, dV.$$

We have assumed, without reducing the level of generality, that $b \geq 0$ (see [11]). Further, as indicated in [11] this minimum is attained at the single positive function $u_* > 0$ in Ω . Let $X_\delta \subset X$ denote a sequence of finite dimensional spaces such that the $H^1(\Omega)$ projections I_{X_δ} onto X_δ converge strongly to the identity operator I_{H^1} . In [11] the convergence of the associated approximates

$$u_\delta \in \arg\text{-min}\{E(v) : v \in X_\delta, \|u\|_{L^2} = 1\} \rightarrow u_*$$

as the projections I_{X_δ} onto X_δ converge to I_{H^1} was shown. In contrary to the infinite dimensional case, the finite dimensional approximation problem has several solutions, but we can always pick a positive one. This sequence of solutions converges to u_* in the L^2 sense as proved in [11]. Further note that the function E is Gateaux differentiable and that, due to convexity, the necessary and the sufficient condition for the existence of the unique positive minimizer is that u_* solves the Euler equation of the Lagrange function associated to (3). The Gateux derivative of $E : X \rightarrow \mathbb{R}$ at the point v is the bounded operator $H_v : X \rightarrow X'$, where $X \subset L^2(\Omega) \subset X'$ is the standard Gelfand triplet. The restriction of the operator H_v

to the operator mapping into $L^2(\Omega)$ is also denoted by H_v and it is the self-adjoint positive definite operator $H_v : \text{Dom}(H_v) \subset L^2(\Omega) \rightarrow L^2(\Omega)$ which verifies

$$(H_v^{1/2}\psi, H_v^{1/2}\phi) = \int_{\Omega} \nabla\psi \cdot \nabla\phi \, dV + \int_{\Omega} (b + \beta v^2) \psi\phi \, dV, \quad \psi, \phi \in X = \text{Dom}(H_v^{1/2}).$$

The square root of the self adjoint operator is taken in the sense of spectral calculus. The Euler equation now reads

$$\langle H_v v - \lambda v, \psi \rangle_{X' \times X} = (H_v^{1/2} v, H_v^{1/2} \psi)_{L^2} - \lambda(v, \psi) = 0, \quad \psi \in X.$$

Note that it can be shown that λ_* is the unique minimum of E on the unit ball and that λ_* is the eigenvalue of the operator H_{u_*} with the eigenvector u_* and λ_* being the simple eigenvalue separated from the rest of the spectrum of H_{u_*} – here it is assumed that u_* is frozen.

Discontinuous Galerkin methods are a suitable choice when dealing with singularly perturbed source problems. This theory is classic and we point to the references [3, 4, 35, 25]. Recently, [19, 30, 29] have presented the first results on using higher order discontinuous Galerkin methods for the approximation of eigenvalue problems.

In comparison, the results for conforming methods are much more abundant, for the source [32] as well as for the linear eigenvalue problem [10, 9] and we point the reader to [32, 8] for lists of further references.

We are interested in approximating the function u_* from a piecewise – as given by a polygonal partition \mathcal{T} of Ω – polynomial, not necessarily continuous, function space X_{δ} . The analysis in [30, 29] is focused on the Schrödinger Hamiltonians with potentials b typical for quantum chemistry computations. In this paper we concentrate on a different class of potentials, which include models of an optical lattice. In [29] exponential convergence of the approximants as well as regularity results on the solution of the Gross-Pitaevskii eigenvalue problem were shown. On the other hand the presence of the optical lattice in the domain Ω makes this a mesoscale-macroscale type of a problem. One possibility to treat such problems is to use two mesh approaches as in [24]. In this paper, we opt for the approach in which the two level structure is inferred by adaptive agglomeration of finite elements as in [2]. A further possibility would be to use a multi-scale finite element method as in [15].

The composite finite element method appeared several times in various contexts. We point out the works of Hackbusch and Sauter [22, 23, 21], which were motivated by the development of multigrid like methods in domains Ω with complicated geometries. In those paper, one can also find extensive references to the history of the method. A complicated domain has features appearing at different scales that needs to be resolved by a sequence of meshes. This is achieved by a sequence of regular meshes which can be transformed in a controlled way (by coarsening or composition of finer level elements) at every level of refinement to resolve a part of the complex geometry. The efficiency of the method as well as its overall feasibility is governed by the skillful and efficient use of restriction and prolongation operators. In the context of higher order discontinuous Galerkin methods, the technique of Hackbusch and Sauter has been extended and developed in [2, 16]. Let

us point out that composite (coarsened) discontinuous spaces are contained as subspaces of discontinuous piecewise polynomial spaces considered by [30] and so the same convergence theory covers the convergence of hp -DGCDFEM methods as well.

3. Discontinuous Galerkin methods

In this section we will present basic results and conventions about discontinuous finite element spaces and their approximation properties. We will then proceed and introduce the composite finite element method of [2].

Any mesh \mathcal{T} used in this section is a subdivision of Ω , with K denoting a generic element. The subdivision \mathcal{T} is constructed via affine mappings $F_K : \hat{K} \rightarrow K$, where \hat{K} is the reference triangle or square. We allow for a maximum of one hanging node per edge and denote by $\mathcal{E}(\mathcal{T})$ and $\mathcal{E}^{\text{int}}(\mathcal{T}) \subset \mathcal{E}(\mathcal{T})$ the set of all edges of the mesh \mathcal{T} and the subset of all interior edges, respectively. Moreover, $\mathcal{E}^{\text{BC}}(\mathcal{T}) \subset \mathcal{E}(\mathcal{T})$ denotes the subset of all boundary edges and h_K, h_E denote the size of the element K and the edge E , respectively.

Now we introduce the polynomial degrees for the approximation in our DG method. For each element K of the mesh \mathcal{T} we associate a polynomial degree $p_K \geq 1$ and introduce the degree vector $\mathbf{p} = \{p_K : K \in \mathcal{T}\}$, with $|\mathbf{p}| = \max_{K \in \mathcal{T}} p_K$. We assume that \mathbf{p} is of bounded local variation in the sense that for any pair of neighbouring elements $K, K' \in \mathcal{T}$, we have

$$\varrho^{-1} \leq \frac{p_K}{p_{K'}} \leq \varrho, \quad (4)$$

where $\varrho \geq 1$ is a constant independent of the particular mesh in a sequence of meshes. For any $E \in \mathcal{E}(\mathcal{T})$, we introduce the edge polynomial degree p_E by

$$p_E = \begin{cases} \max(p_K, p_{K'}), & \text{if } E = \partial K \cap \partial K' \in \mathcal{E}^{\text{int}}(\mathcal{T}), \\ p_K, & \text{if } E = \partial K \cap \partial \Omega \in \mathcal{E}^{\text{BC}}(\mathcal{T}). \end{cases} \quad (5)$$

Hence, for a given partition \mathcal{T} of Ω and a degree vector \mathbf{p} on \mathcal{T} , we define the hp -version of the DG finite element space by

$$V_{\mathbf{p}}(\mathcal{T}) = \left\{ v \in L^2(\Omega) : v|_K \in \mathcal{P}_{p_K}(K), \quad K \in \mathcal{T} \right\}, \quad (6)$$

where $\mathcal{P}_{p_K}(K)$ denotes the polynomial space of order up to p_K on the element K .

Next, we introduce the discrete version of problem (2). Let \mathbf{n}_K denote the outward unit normal on the boundary ∂K of an element K . Given an edge $E \in \mathcal{E}^{\text{int}}(\mathcal{T})$ shared by two elements K^+ and K^- , a vector field \mathbf{v} and a scalar field v , we define the jumps and the averages of \mathbf{v} and v across E by

$$\begin{aligned} \{v\} &= \frac{1}{2} \left(v|_{\bar{K}^+} + v|_{\bar{K}^-} \right), & \llbracket v \rrbracket &= v|_{\bar{K}^+} \cdot \mathbf{n}_K + v|_{\bar{K}^-} \cdot \mathbf{n}_{K'}, \\ \{\mathbf{v}\} &= \frac{1}{2} \left(\mathbf{v}|_{\bar{K}^+} + \mathbf{v}|_{\bar{K}^-} \right), & \llbracket \mathbf{v} \rrbracket &= \mathbf{v}|_{\bar{K}^+} \cdot \mathbf{n}_K + \mathbf{v}|_{\bar{K}^-} \cdot \mathbf{n}_{K'}, \end{aligned} \quad (7)$$

Note that if $E \subset \partial\Omega$, we set $\{\mathbf{v}\} = \mathbf{v}$, $[[\mathbf{v}]] = \mathbf{v} \cdot \mathbf{n}$, $\{v\} = v$ and $[[v]] = v\mathbf{n}$, where \mathbf{n} is the outward unit normal to the boundary $\partial\Omega$.

The DG approximation for problem (2) reads as follows: Find $(\lambda_h, u_h) \in \mathbb{R} \times V_{\mathbf{p}}(\mathcal{T})$ such that

$$B(u_h, v_h) + K_h(u_h, v_h) = \lambda_h(u_h, v_h) \, ds, \quad \forall v_h \in V_{\mathbf{p}}(\mathcal{T}), \quad (8)$$

where the bilinear forms are

$$\begin{aligned} B(w, v) &= \sum_{K \in \mathcal{T}} \int_K (\nabla w \cdot \nabla v + bwv + \beta|w|^2 wv) \, d\mathbf{x} + \sum_{E \in \mathcal{E}(\mathcal{T})} \frac{\gamma p_E^2}{h_E} \int_E [[w]] \cdot [[v]] \, ds \\ K_h(w, v) &= - \sum_{E \in \mathcal{E}(\mathcal{T})} \int_E \{\nabla w\} \cdot [[v]] + \{\nabla v\} \cdot [[w]] \, ds, \end{aligned} \quad (9)$$

and (\cdot, \cdot) denotes the standard linear form. Moreover, γ is the penalty term constant. In this paper, we use the DG norm

$$\|u\|_{\mathcal{T}}^2 = \sum_{K \in \mathcal{T}} \left(\|\nabla u\|_{0,K}^2 + \|b^{1/2}u + \beta^{1/2}|u|u\|_{0,K}^2 \right) + \sum_{E \in \mathcal{E}(\mathcal{T})} \left\| \left(\frac{p_E^2}{h_E} \right)^{1/2} [[u]] \right\|_{0,E}^2, \quad (10)$$

where $\|\cdot\|_{0,K}$ and $\|\cdot\|_{0,E}$ are respectively the L^2 -norm on an element K and on an edge E .

We now define the discrete energy functional

$$E_{\delta}(\psi) = \sum_{K \in \mathcal{T}} \int_K \left(\frac{1}{2} \|\nabla \psi\|^2 + \frac{1}{2} b \psi^2 + \frac{1}{4} \beta \psi^4 \right) \, d\mathbf{x} + \sum_{E \in \mathcal{E}(\mathcal{T})} \frac{\gamma p_E^2}{h_E} \int_E [[\psi]] \cdot [[\psi]] \, ds + K_h(\psi, \psi).$$

The convergence and regularity results from [29] hold under certain smoothness restrictions on the potentials b . Our situation is slightly different. Trapping optical potentials are typically nonnegative functions, $b \geq 0$ almost everywhere.

It was shown in [19] that the symmetric interior penalty forms satisfy the necessary ellipticity and continuity estimates in the DG-norm for any penalty $\gamma > \gamma_0$, where γ_0 is a constant which only depends on shape regularity of \mathcal{T} . Set $\tilde{\delta} = p^2 h^{-1}$, then following the same arguments as in [11, 29], there exists a function $u_{\tilde{\delta}} \in V_{\mathbf{p}}(\mathcal{T})$, such that $(u_{\tilde{\delta}}, 1) \geq 0$ and

$$u_{\tilde{\delta}} \in \arg\text{-min}\{E_{\tilde{\delta}}(v) := B(v, v) + K_h(v, v) : v \in V_{\mathbf{p}}(\mathcal{T})\}. \quad (11)$$

In the following sections we also use the notation

$$\lambda_{\tilde{\delta}} = \inf\{E_{\tilde{\delta}}(v) : v \in V_{\mathbf{p}}(\mathcal{T})\}. \quad (12)$$

Finally, as $\tilde{\delta} = p^2 h^{-1} \rightarrow \infty$ we have that any sequence $u_{\tilde{\delta}}$ which satisfies (11), also verifies $u_{\tilde{\delta}} \rightarrow u$ and $\lambda_{\tilde{\delta}} \rightarrow \lambda$.

4. Implementing discontinuous Galerkin composite finite element method

In this section, we introduce the hp-version of the symmetric interior penalty discontinuous Galerkin composite finite element methods DGCFEM for the numerical approximation of (2). Let \mathcal{T}_{h_j} , $j = 1, \dots, \ell$ be a sequence of nested adaptively refined meshes. This means that every element $\tau_i \in \mathcal{T}_{h_i}$, $i = 1, \dots, \ell-1$ is a parent of a subset of elements which belong to the finer mesh \mathcal{T}_{h_j} , $j = i+1, \dots, \ell$. The mesh \mathcal{T}_{h_1} is assumed to be a conforming overlapping mesh, which does not resolve the computational domain Ω . As a concrete example, Figure 1 depicts a sequence of meshes which ultimately resolve a domain with a curved boundary where a portion of a circular inclusion has a different value of the coefficient functions of the partial differential operator. These features are highlighted using two shades of gray. This means that \mathcal{T}_{h_1} is a mesh which has the granularity that is affordable to solve the problem, but not fine enough to resolve all the details of Ω or to fully represent the coefficient functions of the partial differential operator. Details of the coarsening and refinement algorithm to construct such a sequence of meshes, for the given geometry Ω , can be found in [2, 18]. In order to efficiently transition from one refinement level to the next, one needs an efficient implementation of coarsening and refinement operators. To this end we utilize the regular reference mesh $\widehat{\mathcal{T}}_{h_i}$ and logical meshes $\widetilde{\mathcal{T}}_{h_i}$ which is obtained by moving and/or pruning elements from the reference mesh in order to resolve the features of Ω . Finally, we call \mathcal{T}_{h_j} the physical mesh.

We adopt the following convention, the first overlapping mesh (that is to say overlapping details of the domain Ω , or the discontinuity lines of the coefficient functions) with the granularity which is computationally affordable is called the composite finite element mesh and is denoted as $\mathcal{T}_{CFE} := \mathcal{T}_{h_1}$. We now introduce the main conventions necessary to define a piecewise polynomial space on this domain and with it the discontinuous Galerkin realization of the energy functional.

We denote by $\mathcal{E}_{CFE}^{\text{int}}(\mathcal{T}_{CFE})$ the set of all interior faces of the partition $\mathcal{T}_{CFE}^{\text{int}}$ of Ω , and by $\mathcal{E}_{CFE}^{BC}(\mathcal{T}_{CFE})$ the set of all boundary faces of \mathcal{T}_{CFE} . We emphasize that the term “faces”, of a given composite element $K \in \mathcal{T}_{CFE}$, consists of straight/coplanar $(d-1)$ -dimensional segments of the polygonal/polyhedral domain Ω . The boundary ∂K of an element K and the sets ∂K , $\partial\Omega$ and $\partial K \cap \partial\Omega$ will be identified in a natural way with the corresponding subsets of $\mathcal{E}_{CFE}(\mathcal{T}_{CFE}) \equiv \mathcal{E}_{CFE}^{\text{int}}(\mathcal{T}_{CFE}) \cup \mathcal{E}_{CFE}^{BC}(\mathcal{T}_{CFE})$.

With this notation, we consider the (symmetric) interior penalty hp-DGCFEM for the numerical approximation of (2): find $(\lambda_h, u_h) \in \mathbb{R} \times V_{\mathbf{p}}(\mathcal{T}_{CFE})$ such that

$$B_{CFE}(u_h, v_h) + K_{h,CFE}(u_h, v_h) = \lambda_h(u_h, v_h), \quad \forall v_h \in V_{\mathbf{p}}(\mathcal{T}_{CFE}), \quad (13)$$

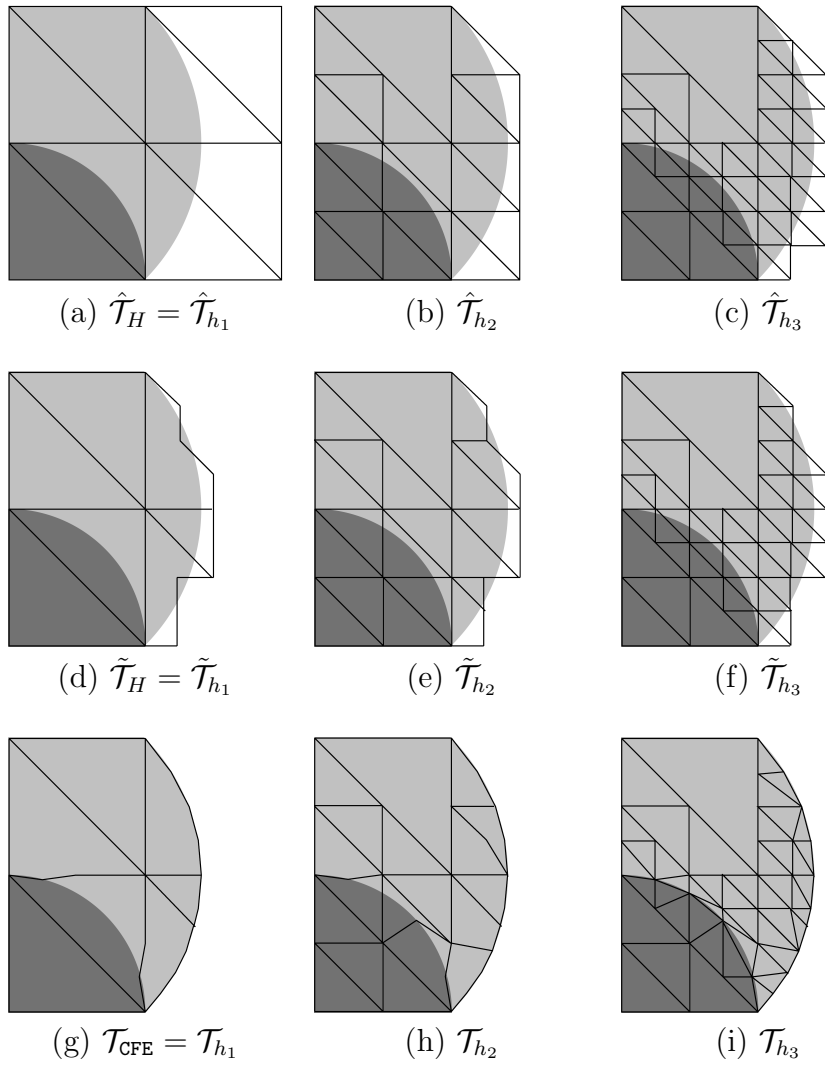


Figure 1: Hierarchy of meshes: (a)–(c) Reference meshes; (d)–(f) Logical Meshes; (g)–(i) Corresponding physical meshes.

where the bilinear forms are

$$\begin{aligned}
B_{\text{CFE}}(w, v) &= \sum_{K \in \mathcal{T}_{\text{CFE}}} \int_K (\nabla w \cdot \nabla v + bwv + \beta|w|^2 wv) \, d\mathbf{x} + \sum_{E \in \mathcal{E}(\mathcal{T}_{\text{CFE}})} \frac{\gamma p_E^2}{h_E^{\text{CFE}}} \int_E \llbracket w \rrbracket \cdot \llbracket v \rrbracket \, ds \\
K_{h, \text{CFE}}(w, v) &= - \sum_{E \in \mathcal{E}_{\text{CFE}}(\mathcal{T})} \int_E \{ \nabla w \} \cdot \llbracket v \rrbracket + \{ \nabla v \} \cdot \llbracket w \rrbracket \, ds,
\end{aligned} \tag{14}$$

and h_E^{CFE} is linked to the size of the fine mesh, as can be seen in the example in Figure 1 subplot (g). The DG CFE norm is defined as

$$\| \| u \| \|_{\mathcal{T}_{\text{CFE}}}^2 = \sum_{K \in \mathcal{T}_{\text{CFE}}} \left(\| \nabla u \|_{0,K}^2 + \| b^{1/2} u + \beta^{1/2} |u| u \|_{0,K}^2 \right) + \sum_{E \in \mathcal{E}(\mathcal{T}_{\text{CFE}})} \left\| \left(\frac{p_E^2}{h_E^{\text{CFE}}} \right)^{1/2} \llbracket u \rrbracket \right\|_{0,E}^2 \tag{15}$$

and we define the CFE realization of the energy functional as

$$\begin{aligned}
E_{\delta_{\text{CFE}}}(\psi) &= \sum_{K \in \mathcal{T}_{\text{CFE}}} \int_K \left(\frac{1}{2} \| \nabla \psi \|^2 + \frac{1}{2} b \psi^2 + \frac{1}{4} \beta \psi^4 \right) \, d\mathbf{x} \\
&\quad + \sum_{E \in \mathcal{E}(\mathcal{T}_{\text{CFE}})} \frac{\gamma p_E^2}{h_E^{\text{CFE}}} \int_E \llbracket \psi \rrbracket \cdot \llbracket \psi \rrbracket \, ds + K_{h, \text{CFE}}(\psi, \psi).
\end{aligned}$$

The notation δ_{CFE} is used for the refinement parameter of the space $V_{\mathbf{p}}(\mathcal{T}_{\text{CFE}})$. This means that if $P_{\delta_{\text{CFE}}} : H^1(\Omega) \rightarrow V_{\mathbf{p}}(\mathcal{T}_{\text{CFE}})$ denotes the orthogonal projection onto $V_{\mathbf{p}}(\mathcal{T})$, then $P_{\delta_{\text{CFE}}} v \rightarrow v$, as $\delta_{\text{CFE}} \rightarrow \infty$. One could think of δ_{CFE} as the dimension of $V_{\mathbf{p}}(\mathcal{T}_{\text{CFE}})$.

Proposition 4.1. *Assume that $b \geq 0$ almost everywhere and $b \in L^q(\Omega)$ for $q > \max\{1, d/2\}$. Then, for composite finite element spaces $V_{\mathbf{p}}(\mathcal{T}_{\text{CFE}})$ such that $\delta_{\text{CFE}} \rightarrow \infty$, there exists a sequence $u_{\delta_{\text{CFE}}} \in V_{\mathbf{p}}(\mathcal{T}_{h_{\text{CFE}}})$ with $(u_{\delta_{\text{CFE}}}, 1) \geq 0$ which verifies*

$$\| u - u_{\delta_{\text{CFE}}} \| \rightarrow 0$$

and $\lambda - \lambda_{\delta_{\text{CFE}}} \rightarrow 0$.

Proof. Our definition of the DG norm is slightly different from the one in [29] and so we outline the proof which is a direct adaptation of the proof of [29, Theorem 1]. We also clearly distinguish the difference of composite finite element spaces from the usual spaces used in [29]. Let $\mathcal{T}_{\text{CFE}} = \mathcal{T}_{h_1}, \dots, \mathcal{T}_{h_l}$ be the sequence of meshes defining the composite finite element space $V_{\mathbf{p}}(\mathcal{T}_{\text{CFE}})$. The coercivity result we need is based on standard results on lifting operators from eg. [31]. The particular form we use was established in [19, Proposition 3.6.] and specialized for composite finite element spaces in [2]. It states that for given $V_{\mathbf{p}}(\mathcal{T}_{\text{CFE}}) \subset V_{\mathbf{p}}(\mathcal{T}_{h_l})$ there exists a constant $\gamma_0 > 1$ and the coercivity constant c_B – and both c_B and γ_0 depend only on the shape regularity of the mesh \mathcal{T}_{h_l} and the level of refinement l necessary to capture all of the details – such that for any $\gamma \geq \gamma_0$ we have

$$c_B \| \| v \| \|_{\mathcal{T}_{\text{CFE}}} \leq c_B \| \| v \| \|_{\mathcal{T}_{h_l}} \leq B_{\text{CFE}}(v, v) + K_{h, \text{CFE}}(v, v).$$

Note that for $v \in V_{\mathbf{p}}(\mathcal{T}_{\text{CFE}})$ we have $|||v|||_{\mathcal{T}_{\text{CFE}}} \leq |||v|||_{\mathcal{T}_{h_l}}$, since the polynomial degree is constant in the composite element and so the restriction of the function onto the composite element is continuous. Let H_u be the self-adjoint operator obtained by evaluating the derivative of the energy E on the solution u and let $u_{\delta_{\text{CFE}}}^*$ be the approximation of the lowest eigenvalue of H_u from the space $V_{\mathbf{p}}(\mathcal{T}_{\text{CFE}})$. For \mathcal{T}_{CFE} fine enough $u_{\delta_{\text{CFE}}}^*$ will be an eigenvector of a simple eigenvalue and $(u_{\delta_{\text{CFE}}}^*, 1) \geq 0$, [29]. Then $|||u_{\delta_{\text{CFE}}}^* - u|||_{\mathcal{T}_{\text{CFE}}} \rightarrow 0$ and $\lambda_{\delta_{\text{CFE}}}^* \rightarrow \lambda$ as $\delta_{\text{CFE}} \rightarrow \infty$ by [17, Theorem 4.4]. As in [29, Equation (31)] we now establish

$$\begin{aligned} c_B |||u_{\delta_{\text{CFE}}} - u_{\delta_{\text{CFE}}}^*|||_{\mathcal{T}_{\text{CFE}}} &\leq (E_{\delta_{\text{CFE}}}(u_{\delta_{\text{CFE}}}) - E(u)) + |\lambda - \lambda_{\delta_{\text{CFE}}}^*| \\ &= (E_{\delta_{\text{CFE}}}(u_{\delta_{\text{CFE}}}) - E_{\delta_{\text{CFE}}}(u)) + |\lambda - \lambda_{\delta_{\text{CFE}}}^*| \end{aligned}$$

Since c_B depends only on the shape regularity of \mathcal{T}_{h_l} the convergence claim

$$|||u_{\delta_{\text{CFE}}} - u_{\delta_{\text{CFE}}}^*|||_{\mathcal{T}_{\text{CFE}}} \rightarrow 0$$

follows by the continuity of $E_{\delta_{\text{CFE}}}$ in the norm $|||\cdot|||_{\mathcal{T}_{\text{CFE}}}$. Moreover, $|||u_{\delta_{\text{CFE}}}^* - u|||_{\mathcal{T}_{\text{CFE}}} \rightarrow 0$ and $|||u_{\delta_{\text{CFE}}} - u_{\delta_{\text{CFE}}}^*|||_{\mathcal{T}_{\text{CFE}}} \rightarrow 0$ imply $|||u - u_{\delta_{\text{CFE}}}|_{\mathcal{T}_{\text{CFE}}} \rightarrow 0$. Finally, starting from \mathcal{T}_{CFE} fine enough we can choose $u_{\delta_{\text{CFE}}}$, so that $(u_{\delta_{\text{CFE}}}, 1) \geq 0$. \square

In order to justify the use of hp -adaptivity as well as to prove finer results on the possibility of exponential convergence rate for the hp adaptive approximation method, the authors of [29] have developed a regularity theory for the solution of Gros-Pitaevskii eigenvalue problem in the presence of potentials b which are singular in finitely many points on Ω , but are otherwise smooth. Our only assumption is that the potential b is an $L^\infty(\Omega)$ function which is also positive in Ω and so, based on standard regularity theory from, we only conclude that $u_* \in H^2(\Omega)$ and that locally u_* can have higher regularity. This indicates that hp adaptive methods can be used to efficiently adapt to the regularity of u_* , see [20, Section 9 and 11]. More detailed analysis of the convergence rate of the composite method is left out for the follow up paper on a-posteriori error estimation.

4.1. Implementation

In order to solve (2), we first compute the first eigenpair for $\beta = 0$ using ARPACK [28] with MUMPS[1]. This is possible because for $\beta = 0$ the nonlinear term vanishes. Such eigenpair is then used as the initial guess for a Picard method outlined in Algorithm 1- The algorithm solve the nonlinear problem with (λ_0, u_0) as the initial guess, \mathbf{A}_m and \mathbf{B} are the nonlinear stiffness matrix computed using \mathbf{u}^m for the nonlinear term and the mass matrix respectively and $\mathbf{tol} = 1\text{e-}9$ in the simulations. The solution of the linear system in Algorithm 1 has been done using PETSc[6, 7] with ILU preconditioner.

Algorithm 1 Picard's method

 $(\lambda_h, u_h) := \text{Picard}(\mathbf{A}, \mathbf{B}, (\lambda_0, u_0), \text{tol})$ $\mathbf{u}^1 := u_0$ $\lambda^1 := \lambda_0$ $m = 1$ **repeat** $\mathbf{u}^{m+1} := \mathbf{A}_m^{-1} \lambda^m \mathbf{B} \mathbf{u}^m$ $\lambda^{m+1} := \frac{(\mathbf{u}^{m+1})^t \mathbf{A}_m \mathbf{u}^{m+1}}{(\mathbf{u}^{m+1})^t \mathbf{B} \mathbf{u}^{m+1}}$ $m := m + 1$ **until** $|\lambda^m - \lambda^{m-1}| < \text{tol}$ $u_h := \mathbf{u}^m$ $\lambda_h := \lambda^m$

In the algorithm (λ_0, u_0) is the initial guess, \mathbf{A}_m and \mathbf{B} are the nonlinear stiffness matrix computed using \mathbf{u}^m for the nonlinear term and the mass matrix respectively and tol is set to 10^{-9} in the simulations. An alternative to Picard's iterations is the more general inverse iteration approach from [26].

5. Numerical results

In this section we present several benchmark results and then compare the efficiency and accuracy of the composite finite element approximation of the ground state with that obtained by the standard discontinuous Galerkin approach. We first consider the harmonic confining potential, and then proceed to analyze the optical lattice potential, which was analyzed in [15].

5.1. A priori convergence for the DG method on problems with smooth potential

In this section we present numerical examples of a priori convergence for a problem with harmonic potential, where $\Omega = (-2, 2)^2$, $b(\mathbf{x}) = x^2 + y^2$ and with $\beta = 100$. Since the analytical form of the smallest eigenpair for such problem is not known, we used as reference the smallest eigenpair computed on a fine mesh using 257×257 nodes and $p = 7$. In the computation Algorithm 1 was used with PETSc on 4 MPI processes, and with block Jacobi preconditioner locally on each process and ILU globally. The relative tolerance for CG in PETSc is set to $1\text{e-}11$ and the tol in Algorithm 1 is set to $1\text{e-}10$. The computed reference eigenvalue is $\lambda_{\text{ref}} = 12.3770867922057$. In Figure 2 we present the behaviour of the relative error for the smallest eigenvalue, i.e.

$$\frac{|\lambda_{\text{ref}} - \lambda_h|}{\lambda_{\text{ref}}},$$

for different choices of p .

In Figures 3 and 4 we have the convergence of the error for the correspondent eigenfunction measured using the DG norm and the L^2 norm, respectively.

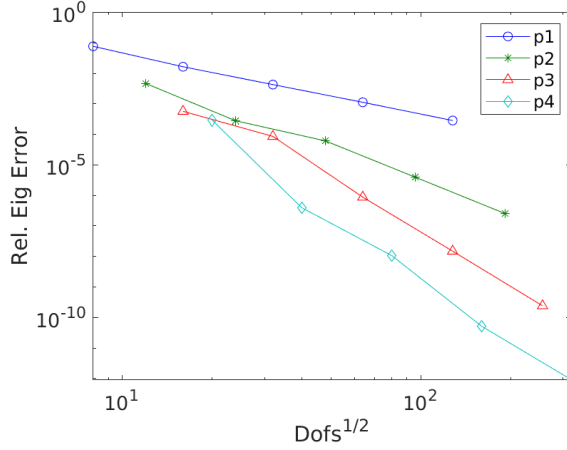


Figure 2: Convergence curves for the relative error for the first eigenvalue with harmonic potential.

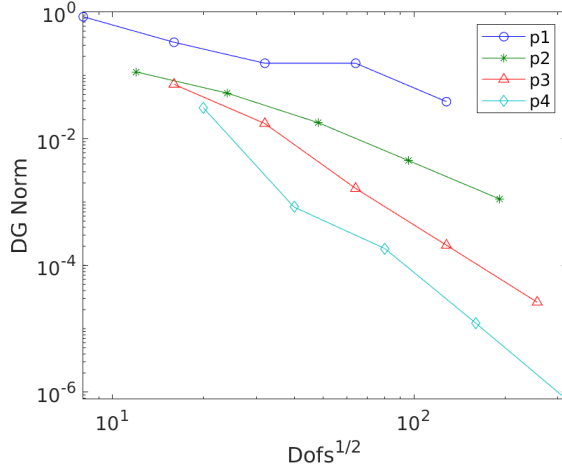


Figure 3: Convergence curves of the DG norm of the error for the first eigenfunction with harmonic potential.

5.2. *A priori convergence for the DG method on problems with discontinuous potential*

In this section we present numerical examples of a priori convergence for the problem in Section 5.2 in [24], where $\Omega = (0, \pi)^2$, $b(\mathbf{x}) = b_0(L(\mathbf{x}/\pi - \frac{\lfloor L\mathbf{x}/\pi \rfloor}{L}))$ and

$$b_0(\mathbf{x}) = \begin{cases} 0, & \mathbf{x} \in (\frac{1}{4}, \frac{3}{4})^2 \\ b_t, & \text{else} \end{cases}$$

with $\beta = 100$. Since the analytical form of the smallest eigenpair for such problem is not known, we used as reference the smallest eigenpair computed on a fine mesh using 257×257 nodes and $p = 7$ using Algorithm 1 with PETSc on 4 MPI processes and with block Jacobi preconditioner locally on each process and ILU globally. The relative tolerance for CG in

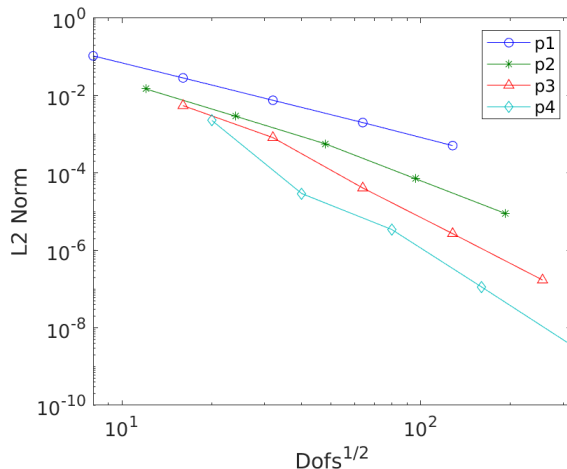


Figure 4: Convergence curves of the $L^2(\Omega)$ norm of the error for the first eigenfunction with harmonic potential.

PETSc is set to 1e-11 and the `tol` in Algorithm 1 is set to 1e-10. The computed reference eigenvalue for $L = 1$ is $\lambda_{\text{ref}} = 51.2326762977125$ and for $L = 2$ is $\lambda_{\text{ref}} = 119.969124220267$. In Figure 5 we present the behaviour of the relative error for the smallest eigenvalue, i.e.

$$\frac{|\lambda_{\text{ref}} - \lambda_h|}{\lambda_{\text{ref}}},$$

for different choices of p and using $L = 1$.

In Figures 6 and 7 we have for $L = 1$ the convergence of the error for the first eigenfunction measured using the DG norm and the $L^2(\Omega)$ norm respectively.

In Figures 8, 9 and 10 we have the convergence of the relative error for the smallest eigenvalue and of the error for the correspondent eigenfunction measured using the DG norm and the $L^2(\Omega)$ norm respectively for the same problem using $L = 2$. The convergence rate increases with p , but only up to a certain point. This is due to the fact that the solution is not completely smooth as a consequence of the discontinuous potential. Therefore increasing p is advantageous until the smoothness level is reached.

5.3. Accuracy of the DG method

As a first test case, we consider the problem in Section 5.2 in [24], where $\Omega = (0, \pi)^2$, $b(\mathbf{x}) = b_0(L(\mathbf{x}/\pi - \frac{\lfloor L\mathbf{x}/\pi \rfloor}{L}))$ and with

$$b_0(\mathbf{x}) = \begin{cases} 0, & \mathbf{x} \in (\frac{1}{4}, \frac{3}{4})^2 \\ b_t, & \mathbf{x} \notin (\frac{1}{4}, \frac{3}{4})^2. \end{cases}$$

In Figures 11–14 we have collected the ground state for $L = 4$, which means that there are 16 potential wells in the domain. Increasing β , the nonlinear part fights against the potential

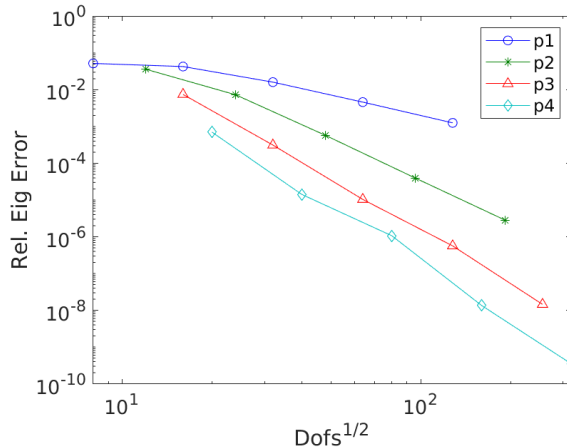


Figure 5: Convergence curves of the relative error for the first eigenvalue when $L = 1$.

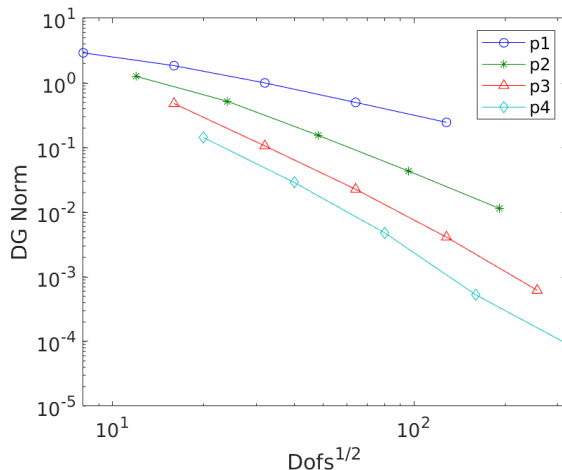


Figure 6: Convergence curves of the DG norm of the error for the first eigenfunction when $L = 1$.

to keep the solution confined and so the solution starts to spread outside the potential wells and over the rest of the domain. To illustrate the variation due to the effect of the nonlinear part, in Figures 15-17 we show the difference between the ground states for $\beta = 1, 10, 100$ and the ground state for $\beta = 0$.

Since the discontinuous term and the nonlinear part are both of order one, this suggests that the solutions are quite smooth and hence a high-order method could be more appropriate. In Figure 18 we tested this idea comparing the error for the eigenvalue using uniform h and uniform p refinements. Due to the smoothness of the solution, uniform p refinement converges exponentially, while uniform h refinement only polynomially. The reference value for λ is computed on a structured mesh of triangles with 257 nodes in each direction and

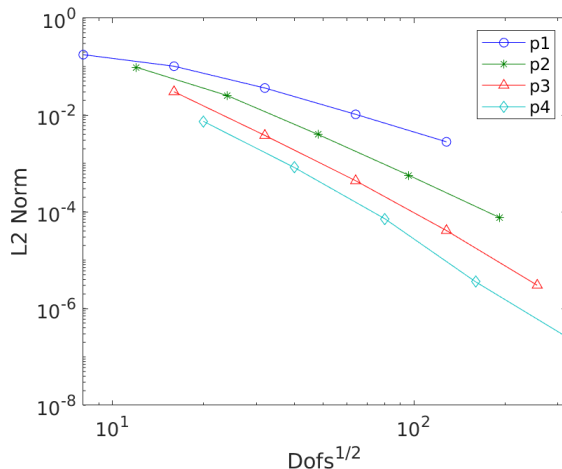


Figure 7: Convergence curves of the $L^2(\Omega)$ norm of the error for the first eigenfunction for $L = 1$.

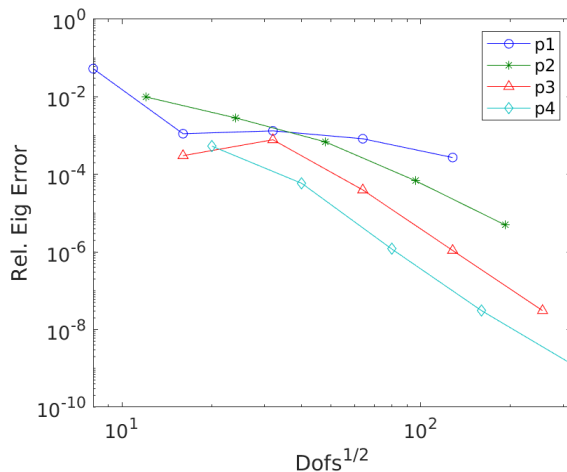


Figure 8: Convergence curves for the relative error for the first eigenvalue for $L = 2$.

order of polynomials 6, such reference value is $\lambda = 74.7570203952487$.

Finally, Figure 19 shows the ground state for $\beta = 100$ and $L = 16$, which results in 256 potential wells.

5.4. Improved accuracy of the CFEDG method based on quadrature

One attractive feature in using the CFEDG method is that the fine level of the method can be used to construct an improved quadrature rule for the coarse level. The fact the potential is piecewise constant impose to standard Gaussian quadrature rules to have a mesh that resolves the interfaces between different values of the potential with its edges, such that in each element the value of the potential is smooth. If the potential is not

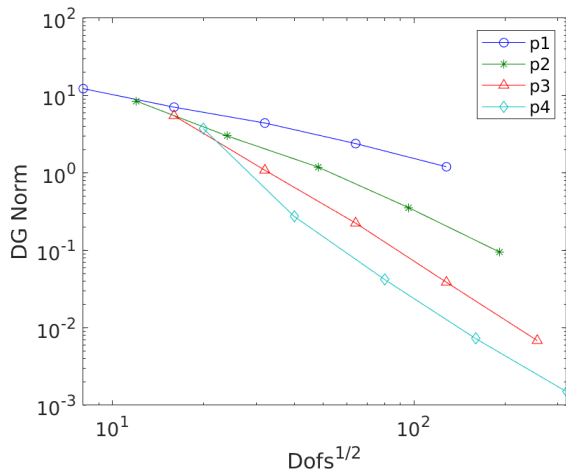


Figure 9: Convergence curves of the DG norm of the error for the first eigenfunction for $L = 2$.

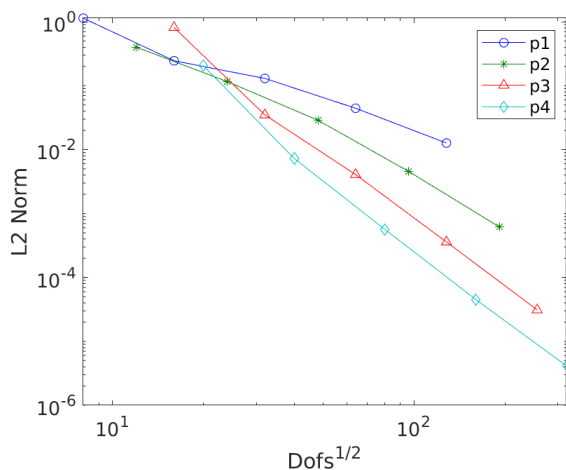


Figure 10: Convergence curves of the $L^2(\Omega)$ norm of the error for the first eigenfunction for $L = 2$.

smooth inside an element, standard Gaussian quadrature rules may not be able to accurately approximate integrals on the element, leading to a possible decrease in the accuracy of the computed solution for the problem. This means that even if the overall solution is quite smooth, a fine scale potential impose for a standard DG method that a fine mesh must be used to keep a good accuracy. This is exactly the opposite of what is found to be more advantageous in Section 5.3, where clearly it is shown that p -methods are superior to h -method for problem (2). This can be avoided using CFEDG, since it is still possible to use a very coarse mesh with possible high p to solve the problem without losing any accuracy in the approximated values for the integrals, simply applying a fine enough mesh to resolve the discontinuities of the potential. The test problem used in this section is the same as in

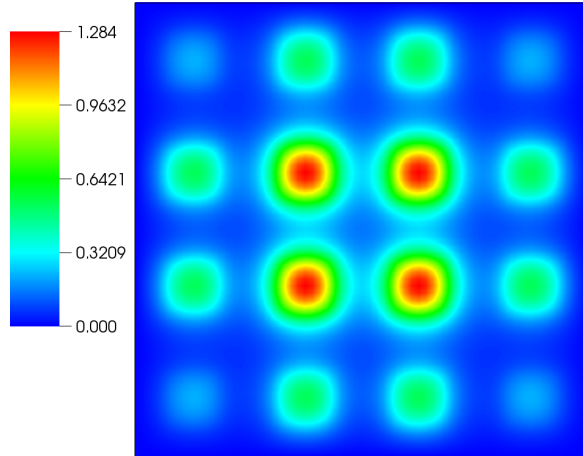


Figure 11: Ground state solution for $\beta = 0$.

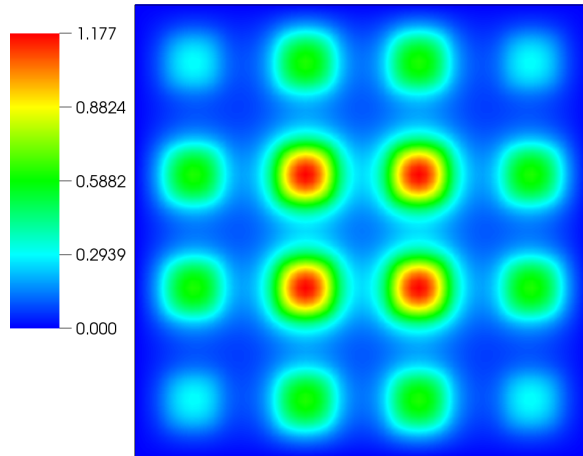


Figure 12: Ground state solution for $\beta = 1$.

Section 5.3, but here we consider different values of $L = 2, 4, 8, 16, 32$. Increasing the value of L , the scale of the potential function reduce and the size of the potential wells decreases. In all simulations a structured coarse mesh of 3×3 nodes is used. The used values of p are from 1 to 4, meaning that the number of degrees of freedom to solve numerically are respectively 24, 48, 80 and 120, since with CFEDG the problem is solved only on the coarse level. In each case the fine level is chosen accordingly to the value of L in order to resolve correctly the

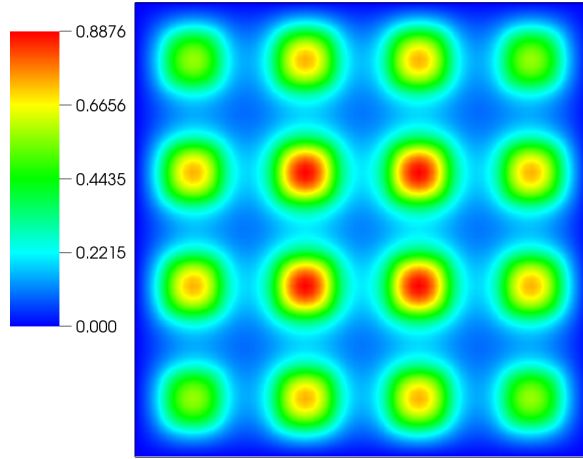


Figure 13: Ground state solution for $\beta = 10$.

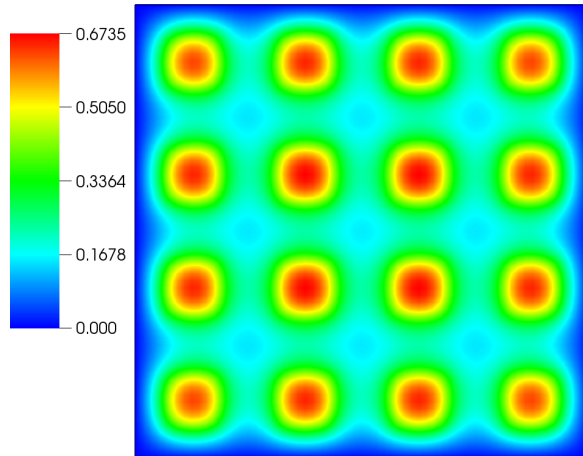


Figure 14: Ground state solution for $\beta = 100$.

potential function. For higher values of L , the fine mesh is finer, increasing the CPU time to compute the entries in the matrices, but not affecting the actual time to solve the discrete problem. For comparison the standard DG method is used with a mesh of 3×3 nodes and the same range of values for p . Clearly such mesh is too coarse to correctly describe the potential for any of the used values of L . In Figure 20, we reported the improvement in the error for the first eigenvalue using the CFEDG method for different values of p and L . The

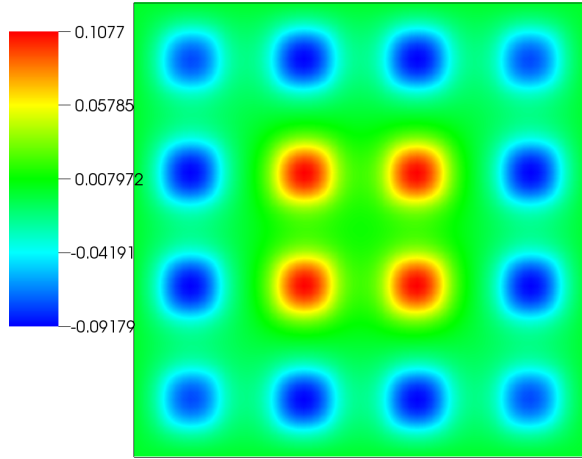


Figure 15: Difference between the ground state for $\beta = 1$ and $\beta = 0$.

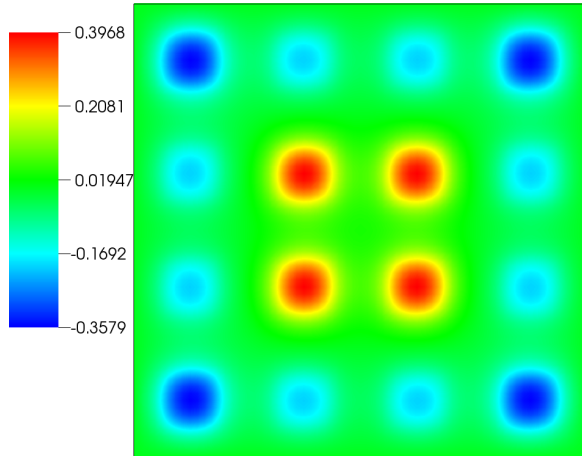


Figure 16: Difference between the ground state for $\beta = 10$ and $\beta = 0$.

improvement is computed as

$$\frac{|\lambda_{\text{ref}} - \lambda_{h,\text{std}}|}{|\lambda_{\text{ref}} - \lambda_{h,\text{CFE}}|},$$

where $\lambda_{h,\text{std}}$ and $\lambda_{h,\text{CFE}}$ are the approximated eigenvalues using, respectively, the standard DG method and the CFEDG method. The reference solution for the eigenvalue λ_{ref} is computed on a structured mesh of triangles with 257 nodes in each direction and with $p = 6$.

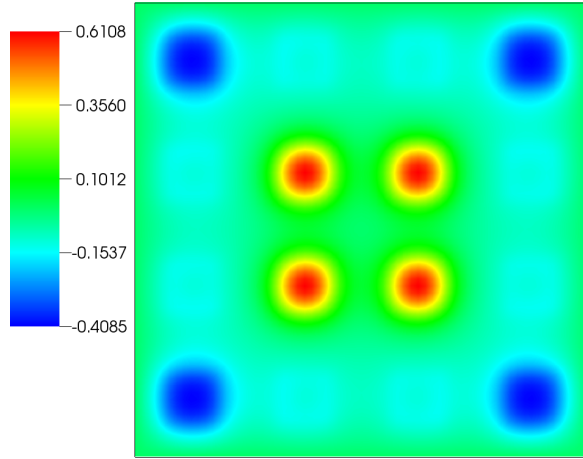


Figure 17: Difference between the ground state for $\beta = 100$ and $\beta = 0$.

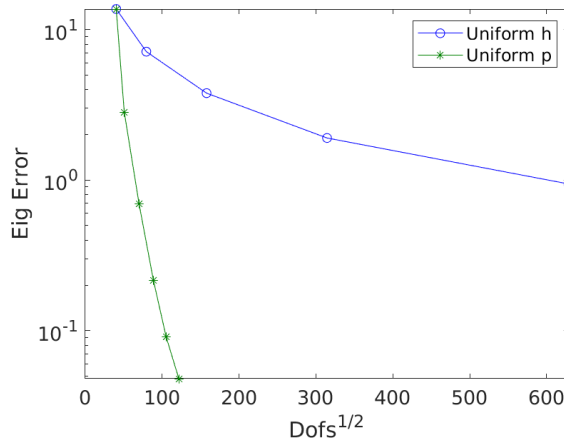


Figure 18: Comparison between the convergence of the computed eigenvalue for $\beta = 100$ using uniform h and uniform p refinements.

It is clear that when the scale of the potential decreases, the accuracy of the CFEDG method compared to the standard DG method increases quite dramatically even if both methods solve numerically problems of same sizes and never exceeding 120 degrees of freedom.

Acknowledgment

The work of L.G. has been supported by the Croatian Science Foundation grant IP-2019-04-6268. We gratefully acknowledge the support.

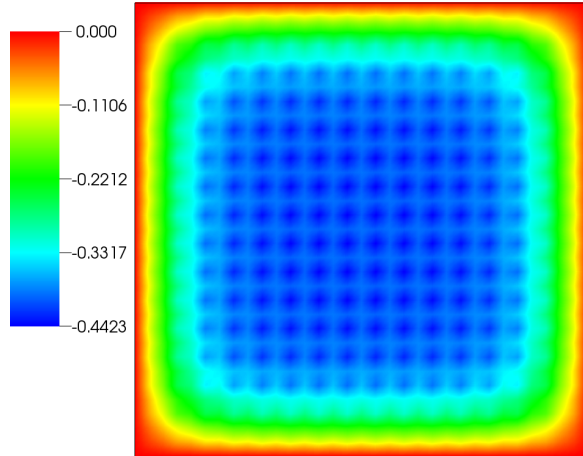


Figure 19: Ground state solution for $\beta = 100$ and $L = 16$.

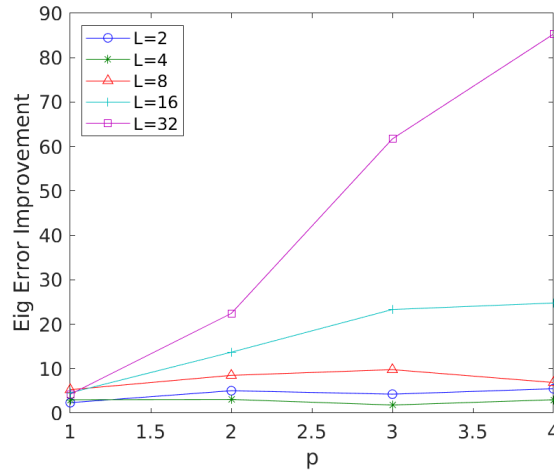


Figure 20: Improvement in the error for the first eigenvalue using the CFEDG method.

References

- [1] P. R. Amestoy, I. S. Duff, and J. Y. L'Excellent. Multifrontal parallel distributed symmetric and unsymmetric solvers. *Computer Methods in Applied Mechanics and Engineering*, 184(2–4):501–520, Apr. 2000.
- [2] P. Antonietti, S. Giani, and P. Houston. hp-version composite discontinuous Galerkin methods for elliptic problems on complicated domains. *SISC*, 35(3):A1417–A1439, 2013.

- [3] D. N. Arnold. An interior penalty finite element method with discontinuous elements. *SIAM J. Numer. Anal.*, 19(4):742–760, 1982.
- [4] D. N. Arnold, F. Brezzi, B. Cockburn, and D. Marini. Discontinuous Galerkin methods for elliptic problems. In *Discontinuous Galerkin methods (Newport, RI, 1999)*, volume 11 of *Lect. Notes Comput. Sci. Eng.*, pages 89–101. Springer, Berlin, 2000.
- [5] P. Bader. Fourier-splitting methods for the dynamics of rotating bose–einstein condensates. *Journal of Computational and Applied Mathematics*, 336:267 – 280, 2018.
- [6] S. Balay, S. Abhyankar, M. F. Adams, J. Brown, P. Brune, K. Buschelman, L. Dalcin, V. Eijkhout, W. D. Gropp, D. Kaushik, M. G. Knepley, L. C. McInnes, K. Rupp, B. F. Smith, S. Zampini, H. Zhang, and H. Zhang. PETSc users manual. Technical Report ANL-95/11 - Revision 3.7, Argonne National Laboratory, 2016.
- [7] S. Balay, W. D. Gropp, L. C. McInnes, and B. F. Smith. Efficient management of parallelism in object oriented numerical software libraries. In E. Arge, A. M. Bruaset, and H. P. Langtangen, editors, *Modern Software Tools in Scientific Computing*, pages 163–202. Birkhäuser Press, 1997.
- [8] D. Boffi. Finite element approximation of eigenvalue problems. *Acta Numer.*, 19:1–120, 2010.
- [9] D. Boffi, R. G. Durán, F. Gardini, and L. Gastaldi. A posteriori error analysis for non-conforming approximation of multiple eigenvalues. *Math. Methods Appl. Sci.*, 40(2):350–369, 2017.
- [10] A. Bonito and A. Demlow. Convergence and optimality of higher-order adaptive finite element methods for eigenvalue clusters. *SIAM J. Numer. Anal.*, 54(4):2379–2388, 2016.
- [11] E. Cancès, R. Chakir, and Y. Maday. Numerical Analysis of Nonlinear Eigenvalue Problems. *J Sci Comput*, 45(1-3):90–117, Oct. 2010.
- [12] S.-L. Chang, H.-S. Chen, B.-W. Jeng, and C.-S. Chien. A spectral-Galerkin continuation method for numerical solutions of the Gross-Pitaevskii equation. *J. Comput. Appl. Math.*, 254:2–16, 2013.
- [13] F. Dalfovo, S. Giorgini, L. P. Pitaevskii, and S. Stringari. Theory of Bose-Einstein condensation in trapped gases. *Rev. Mod. Phys.*, 71:463–512, Apr 1999.
- [14] C. M. Dion and E. Cancès. Ground state of the time-independent Gross–Pitaevskii equation. *Computer Physics Communications*, 177(10):787–798, Nov. 2007.
- [15] D. Elfverson, E. Georgoulis, A. Målqvist, and D. Peterseim. Convergence of a Discontinuous Galerkin Multiscale Method. *SIAM J. Numer. Anal.*, 51(6):3351–3372, Jan. 2013.

- [16] S. Giani. Solving elliptic eigenvalue problems on polygonal meshes using discontinuous Galerkin composite finite element methods. *Applied Mathematics and computation*, 267:618–631, 2015.
- [17] S. Giani. Solving elliptic eigenvalue problems on polygonal meshes using discontinuous galerkin composite finite element methods. *Applied Mathematics and Computation*, 267:618 – 631, 2015.
- [18] S. Giani. An adaptive composite discontinuous Galerkin method for elliptic problems on complicated domains with discontinuous coefficients. *Advances in computational mathematics.*, 46(1):13, February 2020.
- [19] S. Giani, L. Grubišić, H. Hakula, and J. S. Owall. An a posteriori estimator of eigenvalue/eigenvector error for penalty-type discontinuous Galerkin methods. *Appl. Math. Comput.*, 319:562–574, 2018.
- [20] W. Hackbusch. *Elliptic differential equations*, volume 18 of *Springer Series in Computational Mathematics*. Springer-Verlag, Berlin, second edition, 2017. Theory and numerical treatment.
- [21] W. Hackbusch and S. Sauter. A new finite element approach for problems containing small geometric details. volume 34, pages 105–117. 1998. Equadiff 9 (Brno, 1997).
- [22] W. Hackbusch and S. A. Sauter. Adaptive composite finite elements for the solution of PDEs containing non-uniformly distributed micro-scales. In *Proceedings of the International Conference on the Optimization of the Finite Element Approximations (St. Petersburg, 1995)*, volume 8, pages 31–43, 1996.
- [23] W. Hackbusch and S. A. Sauter. Composite finite elements for the approximation of PDEs on domains with complicated micro-structures. *Numer. Math.*, 75(4):447–472, 1997.
- [24] P. Henning, A. Målqvist, and D. Peterseim. Two-Level Discretization Techniques for Ground State Computations of Bose-Einstein Condensates. *SIAM J. Numer. Anal.*, 52(4):1525–1550, Jan. 2014.
- [25] P. Houston, C. Schwab, and E. Süli. Discontinuous *hp*-finite element methods for advection-diffusion-reaction problems. *SIAM J. Numer. Anal.*, 39(6):2133–2163, 2002.
- [26] E. Jarlebring, S. Kvaal, and W. Michiels. An inverse iteration method for eigenvalue problems with eigenvector nonlinearities. *SIAM J. Sci. Comput.*, 36(4):A1978–A2001, 2014.
- [27] T. Kato. *Perturbation theory for linear operators*. Classics in Mathematics. Springer-Verlag, Berlin, 1995. Reprint of the 1980 edition.

- [28] R. B. Lehoucq, D. C. Sorensen, and C. Yang. *ARPACK Users' Guide: Solution of Large Scale Eigenvalue Problems with Implicitly Restarted Arnoldi Methods*. SIAM, 1998.
- [29] Y. Maday and C. Marcati. Analyticity and hp discontinuous Galerkin approximation of nonlinear schrödinger eigenproblems. Technical Report 2019-69, Seminar for Applied Mathematics, ETH Zürich, Switzerland, 2019.
- [30] Y. Maday and C. Marcati. Regularity and hp discontinuous Galerkin finite element approximation of linear elliptic eigenvalue problems with singular potentials. *Math. Models Methods Appl. Sci.*, 29(8):1585–1617, 2019.
- [31] I. Perugia and D. Schötzau. The hp-local discontinuous Galerkin method for low-frequency time-harmonic Maxwell equations. *Math. Comp.*, 72(243):1179–1214, 2003.
- [32] C. Schwab. *p- and hp-finite element methods*. Numerical Mathematics and Scientific Computation. The Clarendon Press, Oxford University Press, New York, 1998. Theory and applications in solid and fluid mechanics.
- [33] A. J. Serna-Reyes and J. Macías-Díaz. Theoretical analysis of a conservative finite-difference scheme to solve a riesz space-fractional gross-pitaevskii system. *Journal of Computational and Applied Mathematics*, page 113413, 2021.
- [34] Y.-S. Wang and C.-S. Chien. A spectral-Galerkin continuation method using Chebyshev polynomials for the numerical solutions of the Gross-Pitaevskii equation. *J. Comput. Appl. Math.*, 235(8):2740–2757, 2011.
- [35] T. P. Wihler, P. Frauenfelder, and C. Schwab. Exponential convergence of the hp-DGFEM for diffusion problems. volume 46, pages 183–205. 2003. *p-FEM2000: p and hp finite element methods—mathematics and engineering practice* (St. Louis, MO).
- [36] J. Williams, R. Walser, C. Wieman, J. Cooper, and M. Holland. Achieving steady-state Bose-Einstein condensation. *Phys. Rev. A*, 57:2030–2036, Mar 1998.
- [37] I. Zapata, F. Sols, and A. J. Leggett. Josephson effect between trapped Bose-Einstein condensates. *Phys. Rev. A*, 57:R28–R31, Jan 1998.